https://doi.org/10.5194/egusphere-2025-3469
Preprint. Discussion started: 29 July 2025

Title: New observations confirm the progressive acidification in the Mozambique Channel

Nicolas Metzl[1], Claire Lo Monaco[1], Aline Tribollet[1], Jean-François Ternon[2], Frédéric Chevallier[3], Marion Gehlen[3]

1 Laboratoire LOCEAN/IPSL, Sorbonne Université-CNRS-IRD-MNHN, Paris, 75005, France
2 MARBEC, Université de Montpellier, CNRS, Ifremer, IRD, 34203 Sète, France
3 Laboratoire LSCE/IPSL, CEA-CNRS-UVSQ, Université Paris-Saclay Gif-sur-Yvette, 91191, France

Correspondence to: Nicolas Metzl (nicolas.metzl@locean.ipsl.fr)

Abstract:

New observations obtained in 2021 and 2022 are presented and used to investigate the trend of the carbonate system (including pH and aragonite saturation state, Ω_{ar}) in the southern sector of the Mozambique Channel. Using historical and new data in April-May we observed an acceleration of the acidification ranging from -0.012 TS.decade^{-1} in 1963-1995 to -0.027 (±0.003) TS.decade^{-1} in 1995-2022. Result from a neural network (FFNN) model for all seasons also suggests faster pH trend in recent decades, -0.011 TS.decade^{-1} over 1985-1995 and -0.018 TS.decade^{-1} over 1995-2022. In May 2022 we estimated Ω_{ar} of 3.49, about 0.3 lower than observed in May 1963 (Ω_{ar} = 3.86). The lowest Ω_{ar} value of 3.23 was evaluated from the FFNN model in September 2023 that corresponds to the hypothetical critical threshold value (3.25) for coral reefs. In 2025 a marine heat wave was observed in this region (sea surface temperature up to 30°C) and data from a BGC-Argo float indicate that sea surface pH was low in January 2025 (pH = 7.95) whereas Ω_{ar} was low in Mach 2025 (Ω_{ar} = 3.2). A projection of the C_T concentrations based on observed anthropogenic CO_2 in subsurface water and emissions scenario, suggests that a risky level for corals (Ω_{ar} < 3) could be reached as soon as year 2034.

Keywords: Ocean Acidification, Decadal Trend, Mozambique Channel

1 Introduction:

The ocean plays a major role in reducing the impact of climate change by absorbing more than 90% of the excess heat in the climate system (Cheng et al., 2025; Forster et al 2025) and about 25% of human released CO_2 (Friedlingstein et al., 2025). The oceanic CO_2 uptake also changes the chemistry of seawater reducing its buffering capacity (Revelle and Suess, 1957) and leading to a process known as ocean acidification (OA) with potential impacts on marine organisms and ecosystems (Fabry et al., 2008; Doney et al., 2009, 2020; Gattuso et al, 2015; Schönberg et al, 2017; Cornwall et al, 2021). Global ocean models or Earth System Models predict that, due to future anthropogenic CO_2 emissions and global warming, the pH could decrease by 0.4 and aragonite saturation state (Ωar) could be as low as 3 in the tropics by 2100 (Hoegh-Guldberg et al, 2007; Kwiatkowski et al, 2020; Jiang et al, 2023; Findlay et al, 2025). However, current global ocean models cannot fully replicate observations and not yet simulating all processes that govern ocean acidification (e.g. seasonal cycles of C_T and A_T, accumulation of C_{ant}, etc...). Long-term observations of the carbonate system are needed to compare and validate model results (Tilbrook et al, 2019).

The first estimate of the decadal pH change based on fugacity of CO_2 (fCO_2) observations in the global ocean (using SOCAT data, Bakker et al, 2014) suggests a decrease of pH ranging between -0.003 TS.decade^{-1} (±0.005) in the North Pacific and -0.024 TS.decade^{-1} (±0.005) in the Indian Ocean over 1981-2011 (Lauvset et al, 2015). Reconstruction methods also based on SOCAT observations

https://doi.org/10.5194/egusphere-2025-3469
Preprint. Discussion started: 29 July 2025

evaluated a global ocean decrease of pH in surface waters of -0.0181 (± 0.0001) TS.decade^{-1} (Iida et al, 2021), −0.0166 (± 0.0010) TS.decade^{-1} (Ma et al, 2023) and −0.017 (± 0.004) TS.decade^{-1} (Chau et al, 2024). These studies also highlighted the regional differences of the pH and aragonite saturation state (Ωar) trends. This calls for dedicated studies at regional scale in order to better interpret the inter-annual to multi-decadal changes of the oceanic carbonate system as the trends and associated uncertainties depend on the data available. Compared to other basins, observations are sparse in the Indian Ocean (Lauvset et al, 2015; Bakker et al, 2016, 2024). However, thanks to a new cruise conducted in 2019, it has been shown that the Mozambique Channel experienced an acceleration of the acidification in recent years, a pH trend of -0.023 TS.decade^{-1} (±0.005) over 1995–2019 (Lo Monaco et al, 2021). In a more recent analysis Chakraborty et al (2024) used several methods, including a high resolution model dedicated to the Indian Ocean and found an acceleration of the pH trend of -0.011 (±0.00).decade^{-1} in 1980–1989 to -0.019 (±0.004).decade^{-1} in 2010–2019.

In this study, we present new data obtained in January 2021 and April-May 2022 in the Mozambique Channel and used the results of a FFNN model (Chau et al, 2024) extended to 2023 to explore the decadal trends of the carbonate system over 1963-2023. We also use these data to validate a projection of the acidification in the near future. To highlight CO_2 source anomalies when the ocean was exceptionally warm, results from a BGC-Argo float in the Mozambique Channel in 2024-2025 are also presented.

2 Data selection and methods

2.1 Data selection

To explore the long-term change of the carbonate system in this region, we selected the fCO_2 SOCAT data, version v2024 (Bakker et al, 2016, 2024). With recent cruises conducted on-board the ship Marion-Dufresne in January 2021 (OISO-31) and April-May 2022 (RESILIENCE) this includes 10 cruises in the Mozambique Channel (Table 1 and Figure 1). Some of these cruises were previously described to analyze the distribution air-sea CO_2 fluxes and pH changes in the Mozambique Basin and the African coastal zone (Metzl et al, 2025b). Here we focus on the data obtained in the southern Mozambique Channel. To complete the shipboard data after 2022 we also used data from a BGC-Argo float (WMO ID 7902123) that was launched onboard R/V Sonne in the Mozambique Channel in late 2024. During some cruises (2004, 2019 and 2021) continuous underway A_T and C_T measurements were also performed (data available in Metzl et al, 2025a). These A_T and C_T data are used to compare and validate results of the pH trends based on fCO_2 data.

Table 1: List of cruises in the Mozambique Channel from SOCAT-v2024 (Bakker et al, 2024).

EXPOCODE	Month	Year	Reference or Principal Investigator
31AR19630216	5	1963	Keeling and Waterman (1968)
316N19950611	6	1995	Key, R.
33RO19990211	2	1999	Wanninkhof, R.
49NZ20031209	12	2003	Murata, A.
35MF20040106(a)	1	2004	Metzl (2009)
06BE20140710	7	2014	Steinhoff, T., Koertzinger, A
33RO20180423	4	2018	Wanninkhof, R., Pierrot, D.
35MV20190405 (a)	4	2019	Lo Monaco et al. (2021)

https://doi.org/10.5194/egusphere-2025-3469
Preprint. Discussion started: 29 July 2025

35MV20210113 (a)	1	2021	Metzl et al. (2025b)
35MV20220420	4	2022	Metzl et al. (2025b)

(a) For these cruises underway A_T C_T data available at https://doi.org/10.17882/102337

Figure 1: Tracks of cruises in the Mozambique Channel in the SOCAT data-base, version v2024 (Bakker et al., 2016; 2024). This includes recent OISO-31 and RESILIENCE cruises in 2021 and 2022. Color code is for Year. Figure produced with ODV (Schlitzer, 2018).

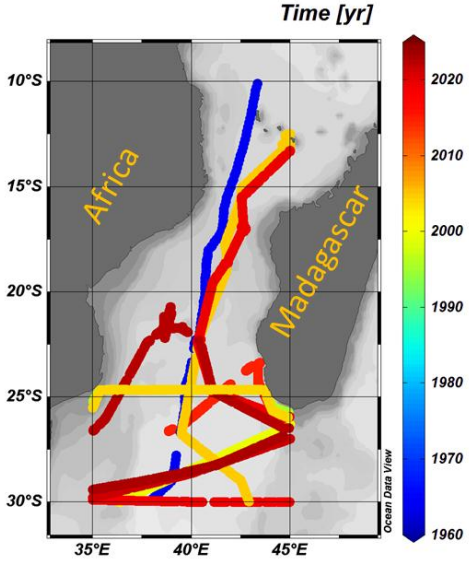

2.2 Methods

The methods for surface underway fCO_2 and A_T C_T measurements were described in previous studies (e.g. Lo Monaco et al, 2021). For fCO_2 measurements during OISO-11 (2004), CLIM-EPARSES (2019), OISO-31 (2021) and RESILIENCE (2022) cruises, sea-surface water was continuously equilibrated with a "thin film" type equilibrator thermostated with surface seawater (Poisson et al., 1993) and xCO2 in the dried gas was measured with a non-dispersive infrared analyzer (NDIR, Siemens Ultramat 6F). Standard gases for calibration (around 280 ppm, 350 ppm and 490 ppm) were measured every 6 hours. The fCO_2 in situ data were corrected for warming using corrections proposed by Copin-Montégut (1988, 1989). Note that when incorporated in the SOCAT data-base, the original fCO2 data are recomputed (Pfeil et al., 2013) using temperature correction from Takahashi et al. (1993). Given the very small difference between equilibrium temperature and sea surface temperature, the fCO_2 data from SOCAT used in this analysis (Bakker et al., 2024) are almost identical (within 1 µatm) to the original fCO_2 values.

During 3 cruises, in January 2004 (OISO-11), April 2019 (CLIM-EPARSES) and January 2021 (OISO-31), A_T and C_T were measured continuously in surface water using a potentiometric titration method (Edmond, 1970) in a closed cell. For calibration, we used the Certified Referenced Materials provided by Pr. A. Dickson (SIO, University of California). Based on repeatability from duplicate analyses of continuous sea surface sampling at the same location (when the ship was stopped) we estimated the accuracy for both A_T and C_T better than 4 µmol.kg^{-1} (Metzl et al, 2025a). The A_T and C_T

https://doi.org/10.5194/egusphere-2025-3469
Preprint. Discussion started: 29 July 2025

data for these cruises are available at the Seanoe platform (https://doi.org/10.17882/102337). These data offered comparisons and validation for the calculations of the carbonate system properties using fCO_2 data and A_T/Salinity relationship.

2.3 Carbonate system calculation and A_T/Salinity relationship

When two of the carbonate system properties are measured (here either fCO_2, A_T or C_T) they can be used to calculate other species and the saturation state of aragonite (Ω_{ar}). Here we used the CO2sys program (version CO2sys_v2.5, Orr et al., 2018) with K1 and K2 dissociation constants from Lueker et al. (2000) and KSO4 constant from Dickson (1990). The total boron concentration is calculated according to Uppström (1974). When using fCO_2 data to derive pH or C_T, one needs A_T concentrations that can be derived from salinity (e.g. Millero et al, 1998). Here we used the A_T/Salinity relationship adapted to the Mozambique Channel (Lo Monaco et al, 2021).

A_T ($\mu mol.kg^{-1}$) = 73.841* Salinity - 291.02 (Eq. 1)

2.4. CMEMS-LSCE-FFNN model

The fCO_2 data are not available each year and only for few seasons (Table 1). To complete the observations we used the results from an ensemble of feed-forward neural network model (CMEMS-LSCE-FFNN or FFNN for simplicity here, Chau et al., 2024). Based on the SOCAT gridded datasets this model composes surface ocean carbonate system fields at 0.25 * 0.25 square degree resolution and monthly scale. The reconstructed fCO_2 is used to derive monthly surface C_T, pH and aragonite and calcite saturation states, as well as air-sea CO_2 fluxes. A full description of the model is presented in Chau et al (2024).

3 Results

3.1 A Repeated line in 2019 and 2022

In April 2019 and 2022 underway measurements were conducted for fCO_2. The measurements of A_T and C_T were also performed in 2019. The tracks of the cruises enabled to select the data obtained along the same track and for the same season in the southern Channel in order to compare the observations three years apart (Figure 2). The mean values over the same latitudinal band (23-26°S) show significant differences between 2019 and 2022 (Table 2). In 2022 the ocean was slightly colder and saltier. Consequently, A_T concentrations were also higher in 2022 but the salinity normalized A_T (N-A_T) were the same with a difference of +1.1 µmol/kg. As expected, due to the CO_2 uptake, the oceanic fCO_2 and C_T concentrations were higher in 2022 and pH was lower. The increase of oceanic fCO_2 over 3 years (+7.9 µatm) was almost the same as in the atmosphere (+7.0 µatm). At constant A_T, salinity and temperature, the observed fCO_2 change would translate in an increase of +4.4 µmol/kg for C_T when we observed an increase of +18 µmol/kg (Table 2). We interpret this difference as being due to the regional circulation. In April 2019 southward currents would import low C_T and A_T whereas in April 2022 northward currents would transport colder and saltier waters with higher C_T and A_T. This reversed circulation is confirmed with the ADCP data recorded during the cruises as well as from the geostrophic currents (Metzl et al, 2022; Ternon et al, 2023).

For pH, the decrease of -0.005 over three years, i.e. -0.0017/yr, is surprisingly close to what is generally observed at global scale and over several decades (-0.017 ±0.004 per decade, Chau et al, 2024). Finally, we note that the difference between 2019 and 2022 measurements is much higher than that obtained when comparing measured and calculated A_T C_T values (Table 2). This confirms the use of fCO_2 data and adapted A_T/S relationship to derive the carbonate system properties in this region (Lo Monaco et al, 2021; Metzl et al, 2025b), and to explore the seasonal cycles and long-term trends described in the next sections.

https://doi.org/10.5194/egusphere-2025-3469
Preprint. Discussion started: 29 July 2025

Table 2: Mean values of underway sea surface observations and their difference obtained along the same track in 2019 and 2022 in the region 23-26°S (see Figure 2). Nb is the number of data. Standard-deviations are in bracket. For 2019 (CLIM-EPARSES cruise), the results from underway A_T-C_T measurements are listed allowing calculation of fCO_2 and pH based on the A_T-C_T pairs which permit comparisons with those derived from fCO_2 measurements.

Cruise Period	Nb	SST °C	SSS -	A_T µmol.kg^{-1}	C_T	fCO_2 µatm	pH TS	Atm. xCO2 ppm
RESILIENCE fCO_2 April 2022	282	26.765 (0.608)	35.423 (0.048)	2324.6 (3.6)	2002.0 (5.0)	394.8 (3.4)	8.047 (0.003)	414.7
CLIM-EPARSES fCO_2 April 2019	294	27.497 (0.341)	35.288 (0.084)	2314.7 (6.2)	1984.0 (7.5)	386.9 (4.9)	8.053 (0.004)	407.5
CLIM-EPARSES A_T-C_T April 2019	70	27.401 (0.390)	35.272 (0.099)	2314.2 (6.7)	1986.1 (8.8)	389.7 (7.4)	8.050 (0.006)	
Difference Method 2019		+0.096	+0.016	+0.5	-2.1	-2.9	+0.002	
Difference 2022-2019		-0.732	+0.135	+10.0	+18.0	+7.9	-0.005	+7.2

https://doi.org/10.5194/egusphere-2025-3469
Preprint. Discussion started: 29 July 2025

Figure 2: Distribution of measured fCO_2 (µatm), calculated C_T (µmol/kg) and calculated pH (TS) along a repeated track in April 2019 (blue) and April 2022 (red) in the southern Mozambique Channel. The dashed red line is for atmospheric fCO_2 in 2022. The underway C_T measurements in 2019 are also shown (open circles) as well as pH calculated using measured A_T and C_T. Average values for the latitudinal band 23-26°S are presented in Table 2.

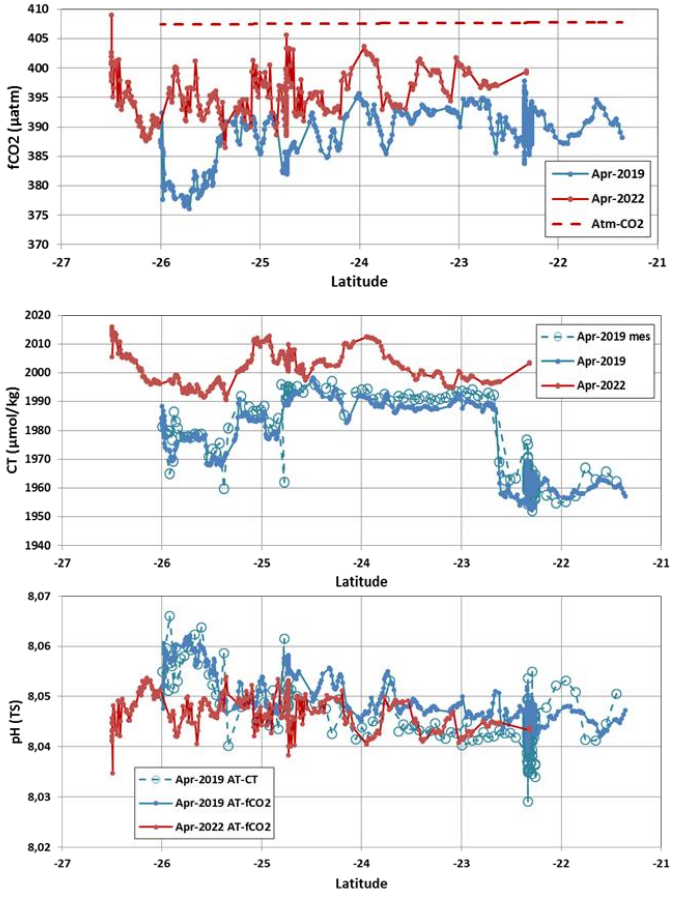

3.2 Seasonal variations

In the Mozambique Channel, where SST presents large seasonal variations (up to 4°C), fCO_2 is mainly controlled by temperature like in the Indian subtropics (e.g. Metzl et al 1998; Takahashi et al, 2002; Bates et al, 2006). In this region, observations are not available for all seasons (Table 1) but the seasonal range derived from the climatology (Fay et al, 2024) or the FFNN model (Chau et al, 2024) is coherent compared to the data (Figure 3). The observations and the models indicate that between January and July fCO_2 decreases by about 50 µatm while pH increases (0.03 to 0.04 units). This is a large signal compared to the expected decadal change (about +20 µatm.decade^{-1} for fCO_2 and -0.017.decade^{-1} for pH); therefore, to derive and interpret the trends, data have to be selected for the same season. As opposed to fCO_2, C_T presents lower concentrations in February-April and higher ones in July-August (Figure 4). When the mixed-layer depth (MLD) is shallow in December-March the decrease of C_T is probably linked to biological activity but this is not clearly quantified (Lo Monaco et al, 2021). The progressive C_T increase of about +30 µmol/kg from March to August is likely driven by vertical mixing when MLD is deeper in summer (Figure 4). This seasonality was well observed from

https://doi.org/10.5194/egusphere-2025-3469
Preprint. Discussion started: 29 July 2025

repeated measurements at stations located along 25°S in June 1995 and December 2003 (Figure S1). In June 1995 when the MLD reached 80 m, C_T concentrations were homogeneous within the MLD layer. The same was true for the anthropogenic CO_2 concentrations (C_{ant}) here evaluated using the TrOCA method (Touratier et al. 2007). On the opposite, in December 2003, when the MLD was shallower, C_T presented a sharp increase within the subsurface layer whereas C_{ant} concentrations were unrealistic in surface seawaters. Although from 1995 to 2003 the C_T concentrations would increase by around +7 µmol/kg due to the anthropogenic CO_2 uptake in that region (Murata et al, 2020; Metzl et al, 2025b), N-C_T (salinity normalized C_T) in June 1995 were almost the same as in December 2003 coherent with the seasonal cycle derived from the climatology (Figure 4).

The seasonal variations of fCO_2 and pH in the Mozambique Channel appear thus linked to both temperature and mixing process with competition between the two drivers (Figure S2). In addition to the rising atmospheric CO_2, these two processes probably also drive inter-annual, decadal and long-term change of fCO_2 and pH in the region as the Indian Ocean experienced a pronounced warming (Cheng et al., 2025). Specifically, in the southern Mozambique Channel the SST has increased by +0.11 ± 0.009 °C per decade since the 1960s (not shown), a signal that should be taken into account when interpreting the decadal trends of carbonate properties and CO_2 fluxes. In January 2025 the SST anomaly reached +1.6°C at 25°S in the Channel.

Figure 3: Seasonal cycle of (a) fCO_2 (µatm) and (b) pH (TS) in the southern Mozambique Channel (24-30°S). Average observations are presented for each cruise (grey circles in 2003-2014, red circles in 2018-2022). The full seasonal cycles are shown for the monthly climatology (reference year 2010, Fay et al, 2024) and for the FFNN model for years 2010 and 2022.

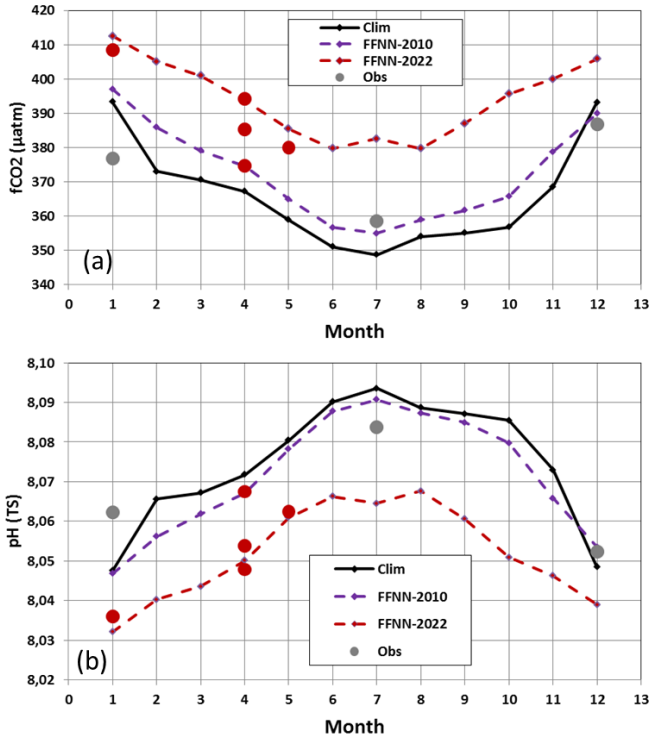

https://doi.org/10.5194/egusphere-2025-3469
Preprint. Discussion started: 29 July 2025

Figure 4: Seasonal cycle of C_T (µmol/kg) in the southern Mozambique Channel (24-30°S). Average observations are presented for each cruise (grey circles in 2003-2014, red circles in 2018-2022). The full seasonal cycles are shown based on the monthly climatology for a reference year 2010 (Fay et al, 2024) and the FFNN-LSCE model for year 2010 (Chau et al, 2024). The mixed-layer depth (MLD in m, blue line) is averaged in this region (from multi-year reprocessed monthly data, ARMOR3D L4, https://doi.org/10.48670/moi-00052, last access 20/4/2025). C_T concentrations are high when MLD is deeper in austral winter.

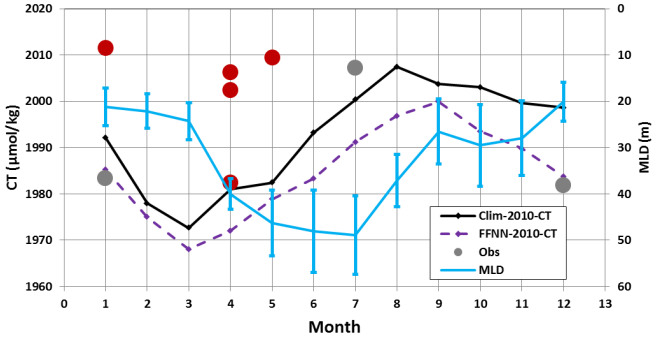

3.3 Trends in the Southern Mozambique Channel (1963-2023)

In this region, the ocean is a permanent CO_2 sink leading to a gradual increase of C_T concentrations and decrease of pH. The air-sea CO_2 flux derived from the FFNN model is on average -0.249 (±0.063) molC/m2/yr (Figure 5) in the range of the climatology (-0.3 molC/m2/yr, Fay et al, 2024). The FFNN model also suggests that the sink increased over 2016-2021 with a perceptible faster increase of C_T (Figure S3).

Figure 5: Time-series of air-sea CO_2 flux (black, negative for ocean sink) and C_T concentration (red) averaged in the southern Mozambique Channel (24-30°S) based on the FFNN-LSCE model over 1985-2023. For C_T, the result is presented with a 36-month running mean. Also shown is the climatological value of the flux for year 2010 in this region (red circle, Fay et al, 2024).

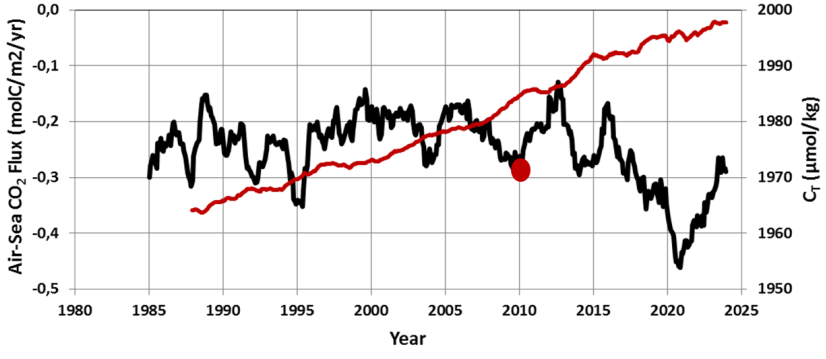

https://doi.org/10.5194/egusphere-2025-3469
Preprint. Discussion started: 29 July 2025

3.3.1 Decadal trend from fCO_2 and A_T C_T data: January 2004 and 2021

We started the analysis of the decadal change by comparing observations obtained in January 2004 and 2021 when data were available for both underway fCO_2, A_T and C_T measurements. The comparison is focused along the tracks occupied in the same region (27-29°S/40-43°E, Figure 6, Table 3). For both cruises the differences between measurements and calculations are in the range of the errors in the CO2sys calculations (errors on measurements and constants K1, K2, Orr et al., 2018). For example, in January 2004 the pH calculated with A_T and C_T measurements was 8.069 against 8.064 when using the fCO_2 data and the A_T/S relationship. In 2021 the pH were respectively 8.030 and 8.032 (Table 3). For C_T the difference between calculated and measured C_T was only 4.4 µmol/kg in 2004 and -1.9 µmol/kg in 2021 when the observed increase over 17 years is around 28 µmol/kg. We noticed that in 2021, the properties present a high variability along the track linked to the presence of eddies. The C_T and A_T concentrations could vary by about 20 to 40 µmol/kg at meso-scale but this has a small impact on calculated fCO_2 and pH, and when properties are averaged along the track (Table 3). For both periods the ocean fCO_2 was close to atmospheric CO_2, i.e. near equilibrium (ΔfCO_2 = -0.04 ±3.11 µatm in 2004 and 0.37 ±10.04 µatm in 2021). Although there were some differences of pH calculated from the two data-sets (underway fCO_2 or A_T C_T data), the estimated pH change of -0.032 or -0.040 over 17 years was large compared to the uncertainty of the CO2sys calculation. This would correspond to a pH trend varying between -0.0019 and -0.0023.yr^{-1}. This comparison of observations in January 2004 and 2021 supports the use of the selected A_T/S relationship for pH calculations based on all fCO_2 data available over 1963–2023 in order to explore the long-term trend described in the next section.

Table 3: Mean values of underway sea surface observations and their difference obtained in the same region (27-29°S/40-43°E) in January 2004 and 2021. Nb is the number of data. Standard-deviations are in bracket. The results are presented for both methods (underway fCO_2 or A_T-C_T measurements) and fCO_2, pH calculated with A_T-C_T pairs compared with those derived from fCO_2 measurements. The last lines are the difference for 2021 minus 2004.

Cruise Method Period	Nb	SST °C	SSS -	A_T µmol.kg^{-1}	C_T	fCO_2 µatm	pH TS	Atm. xCO_2 ppm
OISO-11 fCO_2 January 2004	140	27.293 (0.331)	35.282 (0.050)	2314.2 (3.7)	1978.5 (6.7)	374.7 (3.2)	8.064 (0.002)	374.8
OISO-11 A_T-C_T January 2004	30	27.516 (0.609)	35.248 (0.042)	2315.4 (7.2)	1974.1 (9.8)	368.7 (7.6)	8.069 (0.007)	
OISO-31 fCO_2 January 2021	102	27.825 (0.793)	35.508 (0.118)	2330.9 (8.7)	2006.8 (14.1)	412.5 (10.0)	8.032 (0.008)	412.2
OISO-31 A_T-C_T January 2021	17	27.916 (0.678)	35.515 (0.139)	2326.9 (9.6)	2003.5 (18.7)	414.4 (21.2)	8.030 (0.017)	
Difference 2021-2004								
Underway fCO_2		0.532	0.225	16.7	28.3	37.8	-0.032	37.4
Underway A_T-C_T		0.400	0.267	11.5	29.4	45.7	-0.040	

https://doi.org/10.5194/egusphere-2025-3469
Preprint. Discussion started: 29 July 2025

Figure 6: Distribution of measured or calculated C_T (a, µmol/kg), A_T (b, µmol/kg), fCO_2 (c, µatm) and pH (d, TS) along the same track in January 2004 (black symbols) and January 2021 (grey symbols). In (c) the red lines represent the atmospheric CO_2 in 2004 and 2021. Average values and their differences are presented in Table 3.

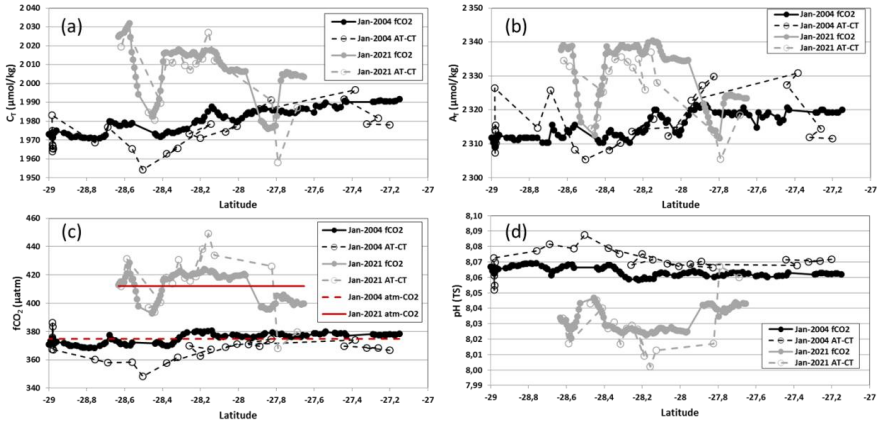

3.3.2 Multi-decadal trends from fCO_2 data (1963-2023)

For long-term trends, we used fCO_2 observations and observations-based reconstructions averaged in the region 24-30°S (Table 4). As the observations are not available for all seasons, we selected the period April-May to calculate the trends from the data (same season for the first and the last cruises in 1963 and 2022) whereas the FFNN model offers information for all seasons. Back in the 1960s, the observations in 1963 indicate that the ocean was a CO_2 sink in May (Figure 7a), the difference of ΔfCO_2 = -32.2 µatm being almost the same as observed in May 2022 (ΔfCO_2 = -32.5 µam). This suggests a strong link between ocean and atmospheric fCO_2 (Figure S4).

For the first observational period, the changes between 1963 and 1995 indicated a pH decrease of -0.040, i.e. -0.0012 TS.yr^{-1}. Over 32 years this pH change was driven by the C_T increase (effect on pH= -0.045), the A_T increase (+0.012) and the warming of 0.95°C (-0.015). Between 1995 and 2022 the observed decrease accelerated to -0.0027 (±0.0003) TS.yr^{-1} (Table 4). In contrast, the neural network suggested smaller pH trends. However, as in the observations, the pH change from the model was faster in recent decades (-0.0018 TS.yr^{-1} over 1995-2022 against -0.0011 TS.yr^{-1} over 1985-1995). The model also suggested different trends depending on the season. The pH trend appeared indeed faster in July (when the ocean CO_2 sink is stronger) than in January or April (Table 4).

The new data in 2021 and 2022 and the FFNN model extended to 2023 confirmed a previous analysis in the Mozambique Channel (Lo Monaco et al, 2021) with a pH trend of -0.0023 TS.yr^{-1} (±0.00048) over 1995–2019. Our new results in the southern Mozambique Channel are also in the range of the pH trends previously evaluated at basin scale in the Indian Ocean, -0.0027 TS.yr^{-1} (±0.0005) over 1991-2011 (Lauvset et al, 2015). High resolution ocean models applied to the northern Indian Ocean also suggest an acceleration of the acidification, with pH trend reaching -0.0019 TS.yr^{-1} (±0.0004) in 2010–2019 (Chakraborty et al, 2024), somehow lower than our estimate based on observations at regional scale in the Mozambique Channel (-0.0027 TS.yr^{-1} ±0.0003 in 1995-2022, Table 4).

https://doi.org/10.5194/egusphere-2025-3469
Preprint. Discussion started: 29 July 2025

Table 4: Trends of properties in the southern Mozambique Channel derived from observations and the FFNN model. For observations, the trends are evaluated for April-May season only. For FFNN, trends are estimated for all seasons or only for January, April and July. Standard-deviations are in bracket.

Method	Period	fCO_2 µatm.yr^{-1}	C_T µmol.kg.yr^{-1}	A_T	pH TS.yr^{-1}
Obs April-May	1963-1995	1.11	0.91	0.52	-0.0012
Obs April-May	1963-2022	1.84 (0.21)	0.69 (0.20)	0.08 (0.13)	-0.0020 (0.0002)
Obs April-May	1995-2022	2.57 (0.30)	0.49 (0.52)	-0.34 (0.22)	-0.0027 (0.0003)
FFNN annual	1985-2023	1.76 (0.05)	0.99 (0.04)	0.02 (0.02)	-0.0017 (0.0001)
FFNN annual	1985-1995	1.15 (0.34)	1.03 (0.29)	0.00 (0.08)	-0.0011 (0.0004)
FFNN annual	1995-2022	1.84 (0.09)	1.10 (0.07)	0.06 (0.03)	-0.0018 (0.0001)
FFNN January	1985-2023	1.61 (0.03)	0.75 (0.07)	0.00 (0.05)	-0.0015 (0.0000)
FFNN April	1985-2023	1.74 (0.03)	1.01 (0.07)	0.03 (0.07)	-0.0017 (0.0000)
FFNN July	1985-2023	1.97 (0.04)	1.17 (0.05)	0.04 (0.02)	-0.0020 (0.0000)

The aragonite saturation state (Ω_{ar}) was lower during austral summer (July-September). In May 1963, we estimated an aragonite saturation state of 3.86 (Figure 7c). It dropped to 3.49 in May 2022, a value close to that observed in July 2014 (3.47). The lowest Ω_{ar} value of 3.23 was identified in September 2023 from the FFNN model. At that period, Ω_{ar} was lower than 3.3 in the south of 20°S in the Mozambique Channel (Figure S5). This is close to the hypothetical critical threshold of Ω_{ar} = 3.25, i.e. a risky level for coral reefs in the ocean claimed by Hoegh-Guldberg et al., (2007). Note that there are reefs know to thrive at Ω_{ar} < 3.25 but that their species composition and coral cover is different than at ambient conditions (e.g. Strahl et al. 2015 in Papua New Guinea; see also review by Camp et al. 2018). With an annual trend of -0.010.yr^{-1} for Ω_{ar} over 1985-2023, a value of 3.3 would be reached in 2060 in summer whereas it was already observed in 2020 in winter with possible consequences on reef species composition and functioning (Tribollet al 2009, 2019; Schönberg et al 2017; Camp et al. 2018; Eyre et al. 2018; Cornwall et al 2021).

Although there are differences depending on the season and the method (in-situ observations, extrapolation of sparse in-situ observations through a FFNN model) all results suggest an acceleration of the acidification in the last few years (Table 4, Figure 7) and a decrease of Ω_{ar} that are mainly driven by the C_T increase through continuous ocean CO_2 uptake (Ma et al, 2023). Given the rapid change of atmospheric CO_2 in the recent years (up to +3.77 ppm.yr^{-1} in 2024, Lan et al, 2025) how the carbonate system will change in the near future in this region and will impact corals reefs that are abundant (from Europa to Mayotte in the Mozambique Chanel) and subject to global warming, marine heat waves (e.g. Mawren et al, 2022; Alaguarda et al. 2022), ocean acidification,

https://doi.org/10.5194/egusphere-2025-3469
Preprint. Discussion started: 29 July 2025

higher frequency of tropical cyclones and anthropogenic pressures (overfishing for instance), remains an important question.

Figure 7: Time-series of fCO_2 (a), pH (b) and Ωar (c) in the southern Mozambique Channel (24-30°S) based on averaged observations (circles) and the FFNN-LSCE model over 1985-2023. In (a) the red line represents the atmospheric CO_2. Available observations are shown for all seasons but the trends (Table 4) evaluated using only April-May data (red circles).

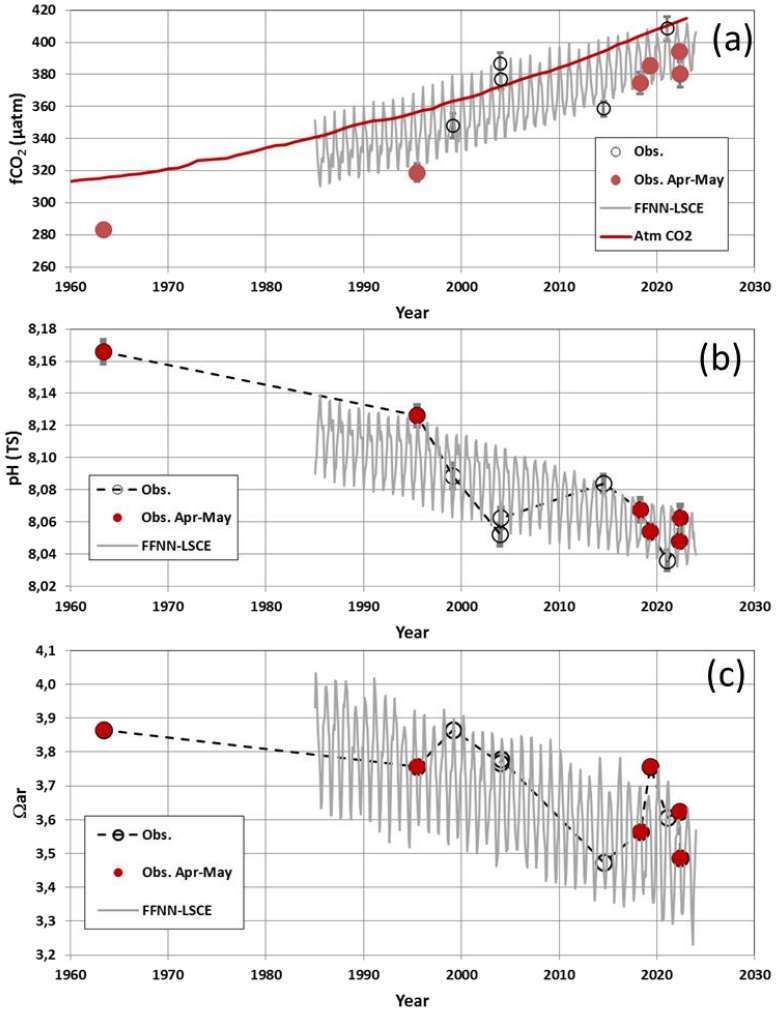

3.4 Projection in the near future

A recent analysis found that the C_{ant} concentrations in subsurface water in the Mozambique Basin were positively related to atmospheric CO_2 with a slope of +0.512 ±0.050 µmol kg^{-1} $µatm^{-1}$ (Metzl et al, 2025b). Here, we assume that this relationship is valid for the southern Mozambique Channel. To reconstruct the past and future change of the carbonate system properties we calculated the C_T concentration over 1960-2100 by correcting C_T for each year using the relationship between C_{ant} and atmospheric CO_2.

https://doi.org/10.5194/egusphere-2025-3469
Preprint. Discussion started: 29 July 2025

$C_T(t) = C_T(t-1) + C_{ant}(t) - C_{ant}(t-1)$ (Eq. 2)

For future atmospheric CO_2, we used two SSP emissions scenarios (Shared Socioeconomic Pathways, Meinshausen et al., 2020), a "high" emission scenario SSP5-8.5 and a stabilization scenario SSP2-4.5 (Figure 8a). To explore the change of the aragonite saturation state, we applied this model (Eq. 2) for August when Ω_{ar} is low. Temperature and salinity were fixed from the climatology in August (SST =22.685 °C; SSS = 35.303) and fCO_2, pH and Ω_{ar} were calculated each year with the C_T A_T pairs using version CO2sys_v2.5 (Orr et al, 2018). The reconstructed C_T, fCO_2, pH and Ω_{ar} for August compared well with the observations (in July) and with the FFNN model in August (Figure 8) indicating that the simulation captured the decadal evolution of the properties. For the future, differences between the two scenarios (SSP5-8.5 and SSP2-4.5) are pronounced after 2030 (Figure 8). For the high scenario the C_T concentrations reaches 2060 µmol/kg in 2040 and pH is as low as 8. In both scenarios, the carbonate ion concentrations dropped below 200 µmol/kg in 2028. As noted above, the aragonite saturation state based on observations was 3.47 in July 2014 (Figure 7c and blue symbol in Figure 8d) and the lowest Ω_{ar} value of 3.23 occurred in August-September 2023 (from the FFNN model, Figure 7c and 8d). The same is estimated in the projection (Figure 7d), close to the critical threshold of Ω_{ar} = 3.25 for tropical coral reefs.

Figure 8: Time-series of (a) atmospheric and oceanic fCO_2, (b) C_T concentrations, (c) pH and (d) Ω_{ar} in the southern Mozambique Channel based on a reconstruction for August for two scenario (SSP85, black line, SSP45 grey lines). Averaged observations (all seasons, July in blue) and the FFNN-LSCE model over 1985-2023 in August (orange) are also shown.

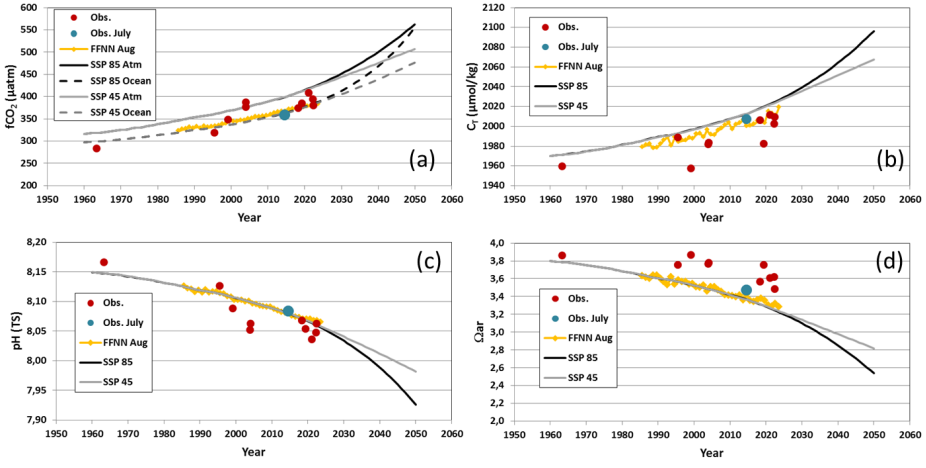

As of January 2025, the atmospheric CO_2 is 426 ppm and 450 ppm should be reached in 2030 in the high scenario SSP5-8.5 (Figure 8a). In a global ocean model it has been suggested that at 450 ppm Ω_{ar} would be around 3 in the South Indian Ocean and the Mozambique Channel, against 4 for pre-industrial Ω_{ar} (Figure 4 in Hoegh-Guldberg et al., 2007). In our simulation, at 450 ppm, Ω_{ar} is equal to 3.13 against 3.8 based on observations in May 1963. Extrapolating our result back in time, we estimated pH at 8.18 and Ω_{ar} equal to 4 at 280 ppm, close to the pre-industrial value estimated from dedicated reconstructions (Lo Monaco et al, 2021) or in global ocean models (Hoegh-Guldberg et al. 2007; Jiang et al, 2023).

Our calculation suggests that for a high emission scenario a risky level for corals (Ω_{ar} < 3) could be reached as soon as year 2034, i.e. in the next 10 years. This calls for maintaining regular carbonate system observations in this region, if possible at all seasons, in order to follow at best their evolution and the potential impact on the channel ecosystem and especially coral reefs in the context of global warming and acidification that will dramatically persist in the near future.

https://doi.org/10.5194/egusphere-2025-3469
Preprint. Discussion started: 29 July 2025

3.5 A large anomaly observed in 2025

As mentioned above, fCO_2 data are relatively sparse in the Mozambique Channel and should be obtained for all seasons. To complete the shipboard observations, biogeochemical (BGC) Argo floats have been developed and successfully used for 10 years for air-sea CO_2 flux estimates and/or acidification especially in the Southern Ocean in the frame of the SOCCOM project (e.g. Sarmiento et al, 2023; Mazloff et al, 2023; Metzl et al, 2025d). The floats record profiles down to 1000 or 2000 m at a 10-day frequency. In November 2024, a BGC-Argo float (WMO ID 7902123) was launched in the Mozambique Channel at 38.51°E/22.65°S (last profile used here recorded on 4th May 2025). Interestingly, the float recorded high temperature in January 2025 (up to 29.8°C, Figure 9a), a signal probably linked to a MHW (Figure S6) that occurred at high frequency in this region (Mawren et al, 2022). Sea surface temperature from reanalysis products suggests a temperature as high as 31°C in this region in January 2025 (Figure S6). Consequently, the sea surface fCO_2 derived from the float pH data reached values above 480 µatm (Figure 9b). This leads to a strong CO_2 source anomaly, in line with CO_2 fluxes anomalies associated to MHW in the South Indian subtropics (e.g. Li et al, 2024). The lowest pH of 7.95 was recorded on 11th January 2025, i.e. lower than the pH derived from the FFNN model (Figure 7b). The aragonite saturation state derived from the BGC-Argo data reached 3.2 in March 2025, the same as that which we estimate in 2025 from the simulation (Figure 8d). The observations from the BGC-Argo offer important information to complement the shipboard data and should be used along with SOCAT data to test constraint data-based products.

Figure 9: Time-series of (a) SST and pH, and (b) fCO_2 and Ω_{ar} in the southern Mozambique Channel based on BGC-Argo data (WMO7902123) in November 2024 to May 2025 (location of data in the insert map). Data from https://www.mbari.org/products/data-repository/, last access 9/5/2025.

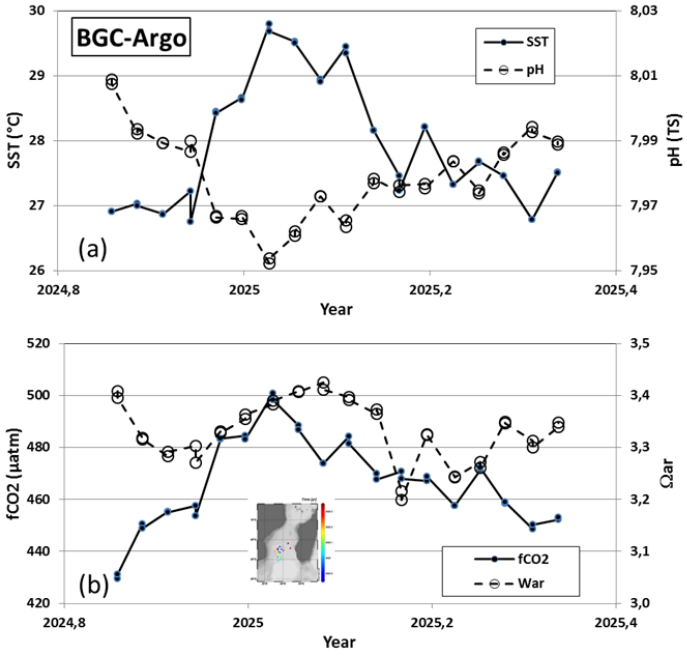

4. Summary and concluding remarks

New observations in 2021 and 2022 and historical fCO_2 data available since 1963 in the Mozambique Channel were used to evaluate the decadal trends of the carbonate system in this region. With adapted A_T/S relationship for this region, we calculated C_T concentrations, pH and Ω_{ar}.

https://doi.org/10.5194/egusphere-2025-3469
Preprint. Discussion started: 29 July 2025

This calculation is first validated with in-situ A_T and C_T measurements obtained in January 2004, April 2019 and January 2021. Based on the data in January 2004 and 2021, we found a pH decrease of -0.032 (using fCO_2 data) and -0.040 (using A_T C_T data) over 17 years. Because the seasonality is large, the decadal trends based on fCO_2 observations in 1963-2022 are evaluated for one season only (April-May). A FFNN model that reconstructed the monthly fields of the carbonate system is also used to investigate the trends for all seasons, but restricted to the period 1985-2023.

In this region where the ocean is a permanent CO_2 sink of -0.25 (±0.06) molC/m2/yr, fCO_2 observations available in April-May translate an acceleration of the acidification ranging from -0.012 TS.decade^{-1} in 1963-1995 to -0.027 (±0.003) TS.decade^{-1} in 1995-2022. Result from the FFNN model for all seasons suggest smaller pH trends but, like in the observations, the decrease of pH was faster in recent decades, -0.011 TS.decade^{-1} over 1985-1995 and -0.018 TS.decade^{-1} over 1995-2022. The FFNN model also suggests a faster trend in austral winter when the ocean CO_2 sink is stronger and when the aragonite saturation state (Ω_{ar}) is low. In May 2022 we estimated Ω_{ar} = 3.49, about 0.3 lower than observed in May 1963 (Ω_{ar} = 3.86). The lowest Ω_{ar} value of 3.23 was evaluated from the FFNN model in September 2023 that corresponds to the potential critical threshold value (3.25) for net reef accretion (Hoegh-Gulberg et al 2007) and could conduct to net reef dissolution (Eyre et al. 2018; Tribollet et al. 2019; Cornwall et al 2021).

A simple reconstruction and projection of the C_T concentrations based on anthropogenic CO_2 in subsurface water and emissions scenario, suggests that the aragonite saturation state could be as low as 3 in the next 10 years. Following a previous work (Lo Monaco et al, 2021), the new data presented here clearly reveal the progressive acidification in the Mozambique Channel and its acceleration in the recent decade with potential impacts on ecosystem including corals reefs areas like at Europa and Bassa de India. In a context where there is no sign of a slowdown in anthropogenic emissions, this already obvious acidification is alarming for the ocean health (Gattuso et al, 2015) and potential feedback on the ocean carbon cycle in general (e.g. Barrett et al, 2025). Understanding and quantifying the future response of phytoplanktonic and reef species in the context of global warming and acidification calls for adapted ocean biogeochemical models (Cornwall et al 2021) to take into account dynamics of bioerosion processes (see Schönberg et al 2017). In the Mozambique Channel, observations are still very sparse and the new observations presented here, including recent BGC-Agro data, offer important information to validate regional and global biogeochemical models that are not yet able to simulate correctly the seasonal cycle and decadal variability of the oceanic carbonate system. We strongly claim for maintaining regular sampling of ocean carbonate system parameters to reduce the model uncertainties and for adapted strategies at both scientific and political actions in the future.

Data availability:

Data used in this study are available in SOCAT (Bakker et al, 2016, www.socat.info) for fCO_2 surface data, in GLODAP (Lauvset et al, 2022a, 2022b, www.glodap.info) for water-column data. The A_T and C_T underway data from OISO and CLIM-EPARSES cruises are available in Seanoe (Metzl et al, 2025c, https://www.seanoe.org, https://doi.org/10.17882/95414 and https://doi.org/10.17882/102337). The BGC-Argo float data with derived carbon parameters are available from SOCCOM (https://soccom.org, https://www.mbari.org/products/data-repository/). The CMEMS-LSCE-FFNN model data are available at E.U. Copernicus Marine Service Information (https://resources.marine.copernicus.eu/products, https://doi.org/10.48670/moi-00047). The Mixed layer depth data are publicly available on the CMEMS website: https://data.marine.copernicus.eu/product/ (Multi Observation Global Ocean ARMOR3D L4 MULTIOBS_GLO_PHY_TSUV_3D_MYNRT_015_012).

Authors contributions:

CLM and NM are co-investigators of the ongoing OISO project. AT was chief scientist of the CLIM-EPARSES 2019 cruise and JFT was chief scientist of the RESILIENCE cruise. MG and FC developed the CMEMS-LSCE-FFNN model and provided the model results. NM started the analysis, wrote the draft of the manuscript and prepared the figures with contributions from all co-authors.

https://doi.org/10.5194/egusphere-2025-3469
Preprint. Discussion started: 29 July 2025

Competing interest: The authors declare that they have no conflict of interest.

Acknowledgments: The OISO program was supported by the French institutes INSU (Institut National des Sciences de l'Univers) and IPEV (Institut Polaire Paul-Emile Victor), OSU Ecce-Terra (at Sorbonne Université), the French programs SOERE/Great-Gases and ICOS-France. We thank the French Oceanographic Fleet for financial and logistic support for the OISO program (https://campagnes.flotteoceanographique.fr/series/228/). The CLIM-EPARSES project was supported by TAAF (Terres Australes et Antarctic Françaises), IRD (Institut de Recherche pour le Développement), Fondation Prince Albert II de Monaco (www.fpa2.org), INSU (Institut National des Sciences de l'Univers), CNRS (Centre National de Recherche Scientifique), Museum National d'Histoire Naturelle (MNHN), UMRs LOCEAN-IPSL, ENTROPIE and LSCE. The RESILIENCE cruise (https://doi.org/10.17600/18001917) was supported by the French National Oceanographic Fleet, by the Belmont Forum Ocean Front Change project, by the ISblue project and by the French National program LEFE (Les Enveloppes Fluides et l'Environnement). We thank the captains and crew of R.R.V. Marion-Dufresne and the staff at IFREMER, GENAVIR and IPEV. We also thank Guillaume Barut, Jonathan Fin and Claude Mignon for their help during the OISO, CLIM-EPARSES and RESILIENCE cruises. The development of the neural network model benefited from funding by the French INSU-GMMC project "PPR-Green-Grog (grant no 5-DS-PPR-GGREOG), the EU H2020 project AtlantOS (grant no 633211), as well as through the Copernicus Marine Environment Monitoring Service (project 83-CMEMS-TAC-MOB). We acknowledge the Southern Ocean Carbon and Climate Observations and Modeling (SOCCOM) Project funded by the National Science Foundation, Division of Polar Programs (NSF PLR-1425989 and OPP-1936222). We thank all colleagues who contributed to the quality control of ocean data made available through GLODAP (www.glodap.info). The Surface Ocean CO_2 Atlas (SOCAT, www.socat.info) is an international effort, endorsed by the International Ocean Carbon Coordination Project (IOCCP), the Surface Ocean Lower Atmosphere Study (SOLAS) to deliver a uniformly quality-controlled surface ocean CO2 database.

References

Alaguarda, D., Brajard, J., Coulibaly, G., Canesi, M., Douville, E., Le Cornec, F., Lelabousse, C. and Tribollet, A.:54 years of microboring community history explored by machine learning in a massive coral from Mayotte (Indian Ocean). Front. Mar. Sci. 9:899398. doi: 10.3389/fmars.2022.899398, 2022

Bakker, D. C. E., B. Pfeil, K. Smith, S. Hankin, A. Olsen, S. R. Alin, C. Cosca, B. Hales, S. Harasawa, A. Kozyr, Y. Nojiri, K. M. O'Brien, U. Schuster, M. Telszewski, B. Tilbrook, C. Wada, J. Akl, L. Barbero, N. Bates, J. Boutin, W.-J. Cai, R. D. Castle, F. P. Chavez, L. Chen, M. Chierici, K. Currie, H. J. W. De Baar, W. Evans, R. A. Feely, A. Fransson, Z. Gao, N. Hardman-Mountford, M. Hoppema, W.-J. Huang, C. W. Hunt, B. Huss, T. Ichikawa, A. Jacobson, T. Johannessen, E. M. Jones, S. Jones, Sara Jutterstrøm, V. Kitidis, A. Körtzinger, S. K. Lauvset, N. Lefèvre, A. B. Manke, J. T. Mathis, L. Merlivat, N. Metzl, P. Monteiro, A. Murata, T. Newberger, T. Ono, G.-H. Park, K. Paterson, D. Pierrot, A. F. Ríos, C.L. Sabine, S. Saito, J. Salisbury, V. V. S. S. Sarma, R. Schlitzer, R. Sieger, I. Skjelvan, T. Steinhoff, K. Sullivan, S. C. Sutherland, T. Suzuki, A. J. Sutton, C. Sweeney, T. Takahashi, J. Tjiputra, N. Tsurushima, S. M. A. C. van Heuven, D. Vandemark, P. Vlahos, D. W. R. Wallace, R. Wanninkhof and A. J. Watson: An update to the Surface Ocean CO2 Atlas (SOCAT version 2). Earth System Science Data, 6, 69-90. doi:10.5194/essd-6-69-2014. 2014

Bakker, D. C. E., Pfeil, B., Landa, C. S., Metzl, N., O'Brien, K. M., Olsen, A., Smith, K., Cosca, C., Harasawa, S., Jones, S. D., Nakaoka, S.-I., Nojiri, Y., Schuster, U., Steinhoff, T., Sweeney, C., Takahashi,

https://doi.org/10.5194/egusphere-2025-3469
Preprint. Discussion started: 29 July 2025

T., Tilbrook, B., Wada, C., Wanninkhof, R., Alin, S. R., Balestrini, C. F., Barbero, L., Bates, N. R., Bianchi, A. A., Bonou, F., Boutin, J., Bozec, Y., Burger, E. F., Cai, W.-J., Castle, R. D., Chen, L., Chierici, M., Currie, K., Evans, W., Featherstone, C., Feely, R. A., Fransson, A., Goyet, C., Greenwood, N., Gregor, L., Hankin, S., Hardman-Mountford, N. J., Harlay, J., Hauck, J., Hoppema, M., Humphreys, M. P., Hunt, C. W., Huss, B., Ibánhez, J. S. P., Johannessen, T., Keeling, R., Kitidis, V., Körtzinger, A., Kozyr, A., Krasakopoulou, E., Kuwata, A., Landschützer, P., Lauvset, S. K., Lefèvre, N., Lo Monaco, C., Manke, A., Mathis, J. T., Merlivat, L., Millero, F. J., Monteiro, P. M. S., Munro, D. R., Murata, A., Newberger, T., Omar, A. M., Ono, T., Paterson, K., Pearce, D., Pierrot, D., Robbins, L. L., Saito, S., Salisbury, J., Schlitzer, R., Schneider, B., Schweitzer, R., Sieger, R., Skjelvan, I., Sullivan, K. F., Sutherland, S. C., Sutton, A. J., Tadokoro, K., Telszewski, M., Tuma, M., Van Heuven, S. M. A. C., Vandemark, D., Ward, B., Watson, A. J., Xu, S., 2016. A multi-decade record of high-quality fCO_2 data in version 3 of the Surface Ocean CO_2 Atlas (SOCAT), Earth Syst. Sci. Data, 8, 383-413, doi:10.5194/essd-8-383-2016.

Bakker, Dorothee C. E.; Alin, Simone R.; Bates, Nicholas; Becker, Meike; Gkritzalis, Thanos; Jones, Steve D.; Kozyr, Alex; Lauvset, Siv K.; Metzl, Nicolas; Nakaoka, Shin-ichiro; O'Brien, Kevin M.; Olsen, Are; Pierrot, Denis; Steinhoff, Tobias; Sutton, Adrienne J.; Takao, Shintaro; Tilbrook, Bronte; Wada, Chisato; Wanninkhof, Rik; Akl, John; Arbilla, Lisandro A.; Arruda, Ricardo; Azetsu-Scott, Kumiko; Barbero, Leticia; Beatty, Cory M.; Berghoff, Carla F.; Bittig, Henry C.; Burger, Eugene F.; Campbell, Katie; Cardin, Vanessa; Collins, Andrew; Coppola, Laurent; Cronin, Margot; Cross, Jessica N.; Currie, Kim I.; Emerson, Steven R.; Enright, Matt P.; Enyo, Kazutaka; Evans, Wiley; Feely, Richard A.; Flohr, Anita; Gehrung, Martina; Glockzin, Michael; González-Dávila, Melchor; Hamnca, Siyabulela; Hartman, Sue; Howden, Stephan D.; Kam, Kitty; Kamb, Linus; Körtzinger, Arne; Kosugi, Naohiro; Lefèvre, Nathalie; Lo Monaco, Claire; Macovei, Vlad A.; Maenner Jones, Stacy; Manalang, Dana; Martz, Todd R.; Mdokwana, Baxolele; Monacci, Natalie M.; Monteiro, Pedro M. S.; Mordy, Calvin; Morell, Julio M.; Murata, Akihiko; Neill, Craig; Noh, Jae-Hoon; Nojiri, Yukihiro; Ohman, Mark; Olivier, Léa; Ono, Tsuneo; Petersen, Wilhelm; Plueddemann, Albert J.; Prytherch, John; Rehder, Gregor; Rutgersson, Anna; Santana-Casiano, J. Magdalena; Schlitzer, Reiner; Send, Uwe; Skjelvan, Ingunn; Sullivan, Kevin F.; T'Jampens, Michiel; Tadokoro, Kazuaki; Telszewski, Maciej; Theetaert, Hannelore; Tsanwani, Mutshutshu; Vandemark, Douglas; van Ooijen, Erik; Veccia, Martín H.; Voynova, Yoana G.; Wang, Hongjie; Weller, Robert A.; Woosley, Ryan J. 2024. Surface Ocean CO2 Atlas Database Version 2024 (SOCATv2024) (NCEI Accession 0293257). [indicate subset used]. NOAA National Centers for Environmental Information. Dataset. https://doi.org/10.25921/9wpn-th28. Last Access 30 June 2024.

Barrett, R. C., Carter, B. R., Fassbender, A. J., Tilbrook, B., Woosley, R. J., Azetsu-Scott, K., et al. (2025). Biological responses to ocean acidification are changing the global ocean carbon cycle. Global Biogeochemical Cycles, 39, e2024GB008358. https://doi.org/10.1029/2024GB008358

Bates, N.R., Pequignet, A.C., and Sabine, C.L.: Ocean carbon cycling in the Indian Ocean: 1. Spatiotemporal variability of inorganic carbon and air-sea CO2 gas exchange. Global Biogeochem. Cycles 20, GB3020. https://doi.org/10.1029/2005GB002491., 2006

Camp E.F., Schoepf, V., Mumby, P. J., Hardtke, L. A., Rodolfo-Metalpa, R., Smith, D. J. and Suggett, D. J.: The Future of Coral Reefs Subject to Rapid Climate Change: Lessons from Natural Extreme Environments. Front. Mar. Sci. 5:4. doi: 10.3389/fmars.2018.00004, 2018.

Chakraborty, K., Joshi, A. P., Ghoshaln P. K., Baduru, B., Valsala, V., Sarma V. V. S. S., Metzl, N., Gehlen, M., Chevallier, F., Lo Monaco, C. Indian Ocean acidification and its driving mechanisms over the last four decades (1980-2019), Global Biogeochemical Cycles, 38, e2024GB008139. https://doi.org/10.1029/2024GB008139, 2024.

Chau, T.-T.-T., Gehlen, M., Metzl, N., and Chevallier, F.: CMEMS-LSCE: a global, 0.25°, monthly reconstruction of the surface ocean carbonate system, Earth Syst. Sci. Data, 16, 121–160, https://doi.org/10.5194/essd-16-121-2024, 2024.

https://doi.org/10.5194/egusphere-2025-3469
Preprint. Discussion started: 29 July 2025

Cheng, L., Abraham, J., Trenberth, K.E. et al. Record High Temperatures in the Ocean in 2024. Adv. Atmos. Sci. 42, 1092–1109. https://doi.org/10.1007/s00376-025-4541-3, 2025

Copin-Montégut, C., 1988. A new formula for the effect of temperature on the partial pressure of CO2 in seawater. Marine Chemistry, 25, 29-37. https://doi.org/10.1016/0304-4203(88)90012-6.

Copin-Montégut, C., 1989. A new formula for the effect of temperature on the partial pressure of CO2 in seawater. Corrigendum. Marine Chemistry, 27, 143-144. https://doi.org/10.1016/0304-4203(89)90034-0.

Cornwall, C.E., S. Comeau, N.A. Kornder, C.T. Perry, R. van Hooidonk, T.M. DeCarlo, M.S. Pratchett, K.D. Anderson, N. Browne, R. Carpenter, G. Diaz-Pulido, J.P. D'Olivo, S.S. Doo, J. Figueiredo, S.A.V. Fortunato, E. Kennedy, C.A. Lantz, M.T. McCulloch, M. González-Rivero, V. Schoepf, S.G. Smithers, & R.J. Lowe, Global declines in coral reef calcium carbonate production under ocean acidification and warming, Proc. Natl. Acad. Sci. U.S.A. 118 (21) e2015265118, doi:10.1073/pnas.2015265118, 2021.

Dickson, A. G., 1990. Standard potential of the reaction: AgCl(s) + ½H2(g) = Ag(s) + HCl(aq), and the standard acidity constant of the ion HSO4– in synthetic sea water from 273.15 to 318.15 K. J. Chem. Thermodyn. 22: 113–127. doi:10.1016/0021-9614(90)90074-Z.

Doney, S.C., Busch, D.S., Cooley, S.R., Kroeker, K.J., 2020. The impacts of ocean acidification on marine ecosystems and reliant human communities. Annu. Rev. Environ. Resour. 45 (1). https://doi.org/10.1146/annurev-environ-012320-083019.

Doney, S.C., Fabry, V.J., Feely, R.A., Kleypas, J.A., 2009. Ocean acidification: The other CO2 problem. Annu. Rev. Mar. Sci. 1 (1), 169–192. https://doi.org/10.1146/annurev.marine.010908.163834.

Edmond, J.M., 1970. High precision determination of titration alkalinity and total carbon dioxide content of sea water by potentiometric titration. Deep-Sea Res. 17, 737–750. https://doi.org/10.1016/0011-7471(70)90038-0.

Eyre, B.D., Cyronak, T., Drupp, P., De Carlo, E.H., Sachs, J.P., Andersson, A.J.: Coral reefs will transition to net dissolving before end of century. Science 359 (6378), 908–911. https://doi.org/10.1126/science.aao1118. 2018

Fabry, V.J., Seibel, B.A., Feely, R.A., Orr, J.C., 2008. Impacts of ocean acidification on marine fauna and ecosystem processes. ICES J. Mar. Sci. 65, 414–432. https://doi.org/10.1093/icesjms/fsn048.

Fay, A. R., Munro, D. R., McKinley, G. A., Pierrot, D., Sutherland, S. C., Sweeney, C., and Wanninkhof, R.: Updated climatological mean ΔfCO2 and net sea–air CO2 flux over the global open ocean regions, Earth Syst. Sci. Data, 16, 2123–2139, https://doi.org/10.5194/essd-16-2123-2024, 2024.

Findlay, H.S., Feely, R.A., Jiang, L.-Q., Pelletier, G. and Bednaršek, N.: Ocean Acidification: Another Planetary Boundary Crossed. Glob Change Biol, 31: e70238. Doi: 10.1111/gcb.70238, 2025

Forster, P. M., Smith, C., Walsh, T., Lamb, W. F., Lamboll, R., Cassou, C., Hauser, M., Hausfather, Z., Lee, J.-Y., Palmer, M. D., von Schuckmann, K., Slangen, A. B. A., Szopa, S., Trewin, B., Yun, J., Gillett, N. P., Jenkins, S., Matthews, H. D., Raghavan, K., Ribes, A., Rogelj, J., Rosen, D., Zhang, X., Allen, M., Aleluia Reis, L., Andrew, R. M., Betts, R. A., Borger, A., Broersma, J. A., Burgess, S. N., Cheng, L., Friedlingstein, P., Domingues, C. M., Gambarini, M., Gasser, T., Gütschow, J., Ishii, M., Kadow, C., Kennedy, J., Killick, R. E., Krummel, P. B., Liné, A., Monselesan, D. P., Morice, C., Mühle, J., Naik, V., Peters, G. P., Pirani, A., Pongratz, J., Minx, J. C., Rigby, M., Rohde, R., Savita, A., Seneviratne, S. I., Thorne, P., Wells, C., Western, L. M., van der Werf, G. R., Wijffels, S. E., Masson-Delmotte, V., and Zhai, P.: Indicators of Global Climate Change 2024: annual update of key indicators of the state of the

https://doi.org/10.5194/egusphere-2025-3469
Preprint. Discussion started: 29 July 2025

climate system and human influence, Earth Syst. Sci. Data Discuss. [preprint], https://doi.org/10.5194/essd-2025-250, in review, 2025.

Friedlingstein, P., O'Sullivan, M., Jones, M. W., Andrew, R. M., Hauck, J., Landschützer, P., Le Quéré, C., Li, H., Luijkx, I. T., Olsen, A., Peters, G. P., Peters, W., Pongratz, J., Schwingshackl, C., Sitch, S., Canadell, J. G., Ciais, P., Jackson, R. B., Alin, S. R., Arneth, A., Arora, V., Bates, N. R., Becker, M., Bellouin, N., Berghoff, C. F., Bittig, H. C., Bopp, L., Cadule, P., Campbell, K., Chamberlain, M. A., Chandra, N., Chevallier, F., Chini, L. P., Colligan, T., Decayeux, J., Djeutchouang, L. M., Dou, X., Duran Rojas, C., Enyo, K., Evans, W., Fay, A. R., Feely, R. A., Ford, D. J., Foster, A., Gasser, T., Gehlen, M., Gkritzalis, T., Grassi, G., Gregor, L., Gruber, N., Gürses, Ö., Harris, I., Hefner, M., Heinke, J., Hurtt, G. C., Iida, Y., Ilyina, T., Jacobson, A. R., Jain, A. K., Jarníková, T., Jersild, A., Jiang, F., Jin, Z., Kato, E., Keeling, R. F., Klein Goldewijk, K., Knauer, J., Korsbakken, J. I., Lan, X., Lauvset, S. K., Lefèvre, N., Liu, Z., Liu, J., Ma, L., Maksyutov, S., Marland, G., Mayot, N., McGuire, P. C., Metzl, N., Monacci, N. M., Morgan, E. J., Nakaoka, S.-I., Neill, C., Niwa, Y., Nützel, T., Olivier, L., Ono, T., Palmer, P. I., Pierrot, D., Qin, Z., Resplandy, L., Roobaert, A., Rosan, T. M., Rödenbeck, C., Schwinger, J., Smallman, T. L., Smith, S. M., Sospedra-Alfonso, R., Steinhoff, T., Sun, Q., Sutton, A. J., Séférian, R., Takao, S., Tatebe, H., Tian, H., Tilbrook, B., Torres, O., Tourigny, E., Tsujino, H., Tubiello, F., van der Werf, G., Wanninkhof, R., Wang, X., Yang, D., Yang, X., Yu, Z., Yuan, W., Yue, X., Zaehle, S., Zeng, N., and Zeng, J.: Global Carbon Budget 2024, Earth Syst. Sci. Data, 17, 965–1039, https://doi.org/10.5194/essd-17-965-2025, 2025.

Gattuso, J.-P., Magnan, A., Billé, R., Cheung, W. W. L., Howes, E. L., Joos, F., Allemand, D., Bopp, L., Cooley, S., Eakin, M., Hoegh-Guldberg, O., Kelly, R. P., Pörtner, H.-O., Rogers, A. D., Baxter, J. M., Laffoley, D., Osborn, D., Rankovic, A., Rochette, J., Sumaila, U. R., Treyer, S., and Turley, C.: Contrasting futures for ocean and society from different anthropogenic CO2 emissions scenarios, Science, 349, aac4722, https://doi.org/10.1126/science.aac4722, 2015.

Hoegh-Guldberg, O., P. J. Mumby, A. J. Hooten, R. S. Steneck, P. Greenfield, E. Gomez, C. D. Harvell, P. F. Sale, A. J. Edwards, K. Caldeira, N. Knowlton, C. M. Eakin, R. Iglesias-Prieto, N. Muthiga, R. H. Bradbury, A. Dubi and M. E. Hatziolos: Coral Reefs Under Rapid Climate Change and Ocean Acidification. Science, 14, 1737-1742, doi:10.1126/science.1152509, 2007

Iida, Y., Takatani, Y., Kojima, A., and Ishii, M.: Global trends of ocean CO2 sink and ocean acidification: an observation based reconstruction of surface ocean inorganic carbon variables, J. Oceanogr., 77, 323–358, https://doi.org/10.1007/s10872-020-00571-5, 2021.

Jiang, L.-Q., Dunne, J., Carter, B. R., Tjiputra, J. F., Terhaar, J., Sharp, J. D., et al., 2023. Global surface ocean acidification indicators from 1750 to 2100. Journal of Advances in Modeling Earth Systems, 15, e2022MS003563. https://doi.org/10.1029/2022MS003563.

Keeling, C. D., Waterman, L. S., 1968. Carbon dioxide in surface ocean waters: 3. Measurements on Lusiad Expedition 1962–1963, *J. Geophys. Res.*, 73(14), 4529– 4541, doi:10.1029/JB073i014p04529.

Kwiatkowski, L., Torres, O., Bopp, L., Aumont, O., Chamberlain, M., Christian, J. R., Dunne, J. P., Gehlen, M., Ilyina, T., John, J. G., Lenton, A., Li, H., Lovenduski, N. S., Orr, J. C., Palmieri, J., Santana-Falcón, Y., Schwinger, J., Séférian, R., Stock, C. A., Tagliabue, A., Takano, Y., Tjiputra, J., Toyama, K., Tsujino, H., Watanabe, M., Yamamoto, A., Yool, A., and Ziehn, T.: Twenty-first century ocean warming, acidification, deoxygenation, and upper-ocean nutrient and primary production decline from CMIP6 model projections, Biogeosciences, 17, 3439–3470, https://doi.org/10.5194/bg-17-3439-2020, 2020.

https://doi.org/10.5194/egusphere-2025-3469
Preprint. Discussion started: 29 July 2025

Lan, X., Tans, P. and K.W. Thoning: Trends in globally-averaged CO2 determined from NOAA Global Monitoring Laboratory measurements. Version Monday, 05-May-2025 16:38:58 MDT https://doi.org/10.15138/9N0H-ZH07, 2025

Lauvset, S. K., Gruber, N., Landschützer, P., Olsen, A., and Tjiputra, J.: Trends and drivers in global surface ocean pH over the past 3 decades. Biogeosciences, 12, 1285-1298, doi:10.5194/bg-12-1285-2015, 2015

Lauvset, S. K., Lange, N., Tanhua, T., Bittig, H. C., Olsen, A., Kozyr, A., Alin, S., Álvarez, M., Azetsu-Scott, K., Barbero, L., Becker, S., Brown, P. J., Carter, B. R., da Cunha, L. C., Feely, R. A., Hoppema, M., Humphreys, M. P., Ishii, M., Jeansson, E., Jiang, L.-Q., Jones, S. D., Lo Monaco, C., Murata, A., Müller, J. D., Pérez, F. F., Pfeil, B., Schirnick, C., Steinfeldt, R., Suzuki, T., Tilbrook, B., Ulfsbo, A., Velo, A., Woosley, R. J., and Key, R. M.: GLODAPv2.2022: the latest version of the global interior ocean biogeochemical data product, Earth Syst. Sci. Data, 14, 5543–5572, https://doi.org/10.5194/essd-14-5543-2022, 2022a.

Lauvset, Siv K.; Lange, Nico; Tanhua, Toste; Bittig, Henry C.; Olsen, Are; Kozyr, Alex; Alin, Simone R.; Álvarez, Marta; Azetsu-Scott, Kumiko; Barbero, Leticia; Becker, Susan; Brown, Peter J.; Carter, Brendan R.; Cotrim da Cunha, Leticia; Feely, Richard A.; Hoppema, Mario; Humphreys, Matthew P.; Ishii, Masao; Jeansson, Emil; Jiang, Li-Qing; Jones, Steve D.; Lo Monaco, Claire; Murata, Akihiko; Müller, Jens Daniel; Pérez, Fiz F.; Pfeil, Benjamin; Schirnick, Carsten; Steinfeldt, Reiner; Suzuki, Toru; Tilbrook, Bronte; Ulfsbo, Adam; Velo, Antón; Woosley, Ryan J.; Key, Robert M. (2022). Global Ocean Data Analysis Project version 2.2022 (GLODAPv2.2022) (NCEI Accession 0257247). [indicate subset used]. NOAA National Centers for Environmental Information. [Dataset]. https://doi.org/10.25921/1f4w-0t92. Last Access [4 June 2025], 2022b

Li, C., Burger, F. A., Raible, C. C., and Frölicher, T. L.: Observed regional impacts of marine heatwaves on sea-air CO2 exchange. Geophysical Research Letters, 51, e2024GL110379. https://doi.org/10.1029/2024GL110379, 2024

Lo Monaco, C., Metzl, N., Fin, J., Mignon, C., Cuet, P., Douville, E., Gehlen, M., Trang Chau, T.T., Tribollet, A., 2021. Distribution and long-term change of the sea surface carbonate system in the Mozambique Channel (1963-2019), Deep-Sea Research Part II, https://doi.org/10.1016/j.dsr2.2021.104936.

Lueker, T.J., Dickson, A.G., Keeling, C.D., 2000. Ocean pCO(2) calculated from dissolved inorganic carbon, alkalinity, and equations for K-1 and K-2: validation based on laboratory measurements of CO2 in gas and seawater at equilibrium. Marine Chemistry 70, 105-119. https://doi.org/10.1016/S0304-4203(00)00022-0.

Ma, D., Gregor, L., and Gruber, N.: Four decades of trends and drivers of global surface ocean acidification. Global Biogeochemical Cycles, 37, e2023GB007765. 10.1029/2023GB007765, 2023

Mawren, D., Hermes, J. & Reason, C.J.C. Marine heatwaves in the Mozambique Channel. Clim Dyn (2022). https://doi.org/10.1007/s00382-021-05909-3

Mazloff, M. R., Verdy, A., Gille, S. T., Johnson, K. S., Cornuelle, B. D., and Sarmiento, J.: Southern Ocean acidification revealed by biogeochemical-Argo floats. Journal of Geophysical Research: Oceans, 128, e2022JC019530. https://doi.org/10.1029/2022JC019530, 2023.

Meinshausen, M., Nicholls, Z. R. J., Lewis, J., Gidden, M. J., Vogel, E., Freund, M., et al.: The shared socioeconomic pathway (SSP) greenhouse gas concentrations and their extensions to 2500. Geoscientific Model Development, 13(8), 3571–3605. https://doi.org/10.5194/gmd-13-3571-2020, 2020.

https://doi.org/10.5194/egusphere-2025-3469
Preprint. Discussion started: 29 July 2025

Metzl, N., Louanchi, F., and Poisson, A.: Seasonal and interannual variations of sea surface carbon dioxide in the subtropical indian ocean. Mar. Chem. 60, 131–146. https://doi.org/10.1016/S0304-4203(98)00083-8., 1998

Metzl, N.: Decadal increase of oceanic carbon dioxide in Southern Indian Ocean surface waters (1991–2007), Deep-Sea Res. Pt. II, 56, 607–619, https://doi.org/10.1016/j.dsr2.2008.12.007, 2009.

Metzl, N., Lo Monaco, C., Tribollet, A., and Kartavtseff A.. CLIM-EPARSES 1 cruise: S-ADCP data. SEANOE. https://doi.org/10.17882/89702, 2022

Metzl, N., Fin, J., Lo Monaco, C., Mignon, C., Alliouane, S., Bombled, B., Boutin, J., Bozec, Y., Comeau, S., Conan, P., Coppola, L., Cuet, P., Ferreira, E., Gattuso, J.-P., Gazeau, F., Goyet, C., Grossteffan, E., Lansard, B., Lefèvre, D., Lefèvre, N., Leseurre, C., Petton, S., Pujo-Pay, M., Rabouille, C., Reverdin, G., Ridame, C., Rimmelin-Maury, P., Ternon, J.-F., Touratier, F., Tribollet, A., Wagener, T., and Wimart-Rousseau, C.: An updated synthesis of ocean total alkalinity and dissolved inorganic carbon measurements from 1993 to 2023: the SNAPO-CO2-v2 dataset, Earth Syst. Sci. Data, 17, 1075–1100, https://doi.org/10.5194/essd-17-1075-2025, 2025a.

Metzl, N., C. Lo Monaco, G. Barut and J.-F. Ternon: Contrasting trends of the ocean CO2 sink and pH in the Agulhas current system and the Mozambique Basin, South-Western Indian Ocean (1963-2023). Deep Sea Research Part II: Topical Studies in Oceanography, 105459, https://doi.org/10.1016/j.dsr2.2025.105459, 2025b

Metzl, N., Fin, J., Lo Monaco, C., Mignon, C., Alliouane, S., Bombled B., Boutin, J., Bozec, Y., Comeau, S., Conan, P., Coppola, L., Cuet, P., Ferreira, E., Gattuso, J.-P., Gazeau, F., Goyet, C., Grossteffan, E., Lansard, B., Lefèvre, D., Lefèvre, N., Leseurre, C., Lombard, F., Petton, S., Pujo-Pay, M., Rabouille, C., Reverdin, G., Ridame, C., Rimmelin-Maury, P., Ternon, J.-F., Touratier, F., Tribollet, A., Wagener, T., and Wimart-Rousseau, C.: An updated synthesis of ocean total alkalinity and dissolved inorganic carbon measurements from 1993 to 2023: the SNAPO-CO2-v2 dataset. SEANOE. [dataset], Last Access [4 June 2025], https://doi.org/10.17882/102337, 2025c.

Metzl, N., C. Lo Monaco, C. Leseurre, G. Barut, G. Reverdin, C. Ridame, and L. Talley: Anthropogenic CO2 and acidification in the Southern Indian Ocean: combining ship-board and BGC-Argo float data, Glob. Biog. Cycl., in rev. 2025GB008606. 2025d

Millero, F. J., Lee, K., Roche, M.: Distribution of alkalinity in the surface waters of the major oceans. Mar. Chem. 60, 111–130. https://doi.org/10.1016/S0304-4203(97)00084-4, 1998

Murata, A., Kumamoto, Y., Sasaki, K., Watanabe, S., and Fukasawa, M.:Decadal increases in anthropogenic CO2 along 20◦S in the SouthSouth Indian ocean. J. Geophys. Res. 115, C12055. https://doi.org/10.1029/2010JC006250, 2010

Pfeil, B., Olsen, A., Bakker, D. C. E., Hankin, S., Koyuk, H., Kozyr, A., Malczyk, J., Manke, A., Metzl, N., Sabine, C. L., Akl, J., Alin, S. R., Bates, N., Bellerby, R. G. J., Borges, A., Boutin,J., Brown, P. J., Cai, W.-J., Chavez, F. P., Chen, A., Cosca, C., Fassbender, A. J., Feely, R. A., González-Dávila, M., Goyet, C., Hales, B., Hardman-Mountford, N., Heinze, C., Hood, M., Hoppema, M., Hunt, C. W., Hydes, D., Ishii, M., Johannessen, T., Jones, S. D., Key, R. M., Körtzinger, A., Landschützer, P., Lauvset, S. K., Lefèvre, N., Lenton, A., Lourantou, A., Merlivat, L., Midorikawa, T., Mintrop, L., Miyazaki, C., Murata, A., Nakadate, A., Nakano, Y., Nakaoka, S., Nojiri, Y., Omar, A. M., Padin, X. A., Park, G.-H., Paterson, K., Perez, F. F., Pierrot, D., Poisson, A., Ríos, A. F., Santana-Casiano, J. M., Salisbury, J., Sarma, V. V. S. S., Schlitzer, R., Schneider, B., Schuster, U., Sieger, R., Skjelvan, I., Steinhoff, T., Suzuki, T., Takahashi, T., Tedesco, K., Telszewski, M., Thomas, H., Tilbrook, B., Tjiputra, J., Vandemark, D., Veness, T., Wanninkhof, R., Watson, A. J., Weiss, R., Wong, C. S., Yoshikawa-Inoue, H.: A uniform, quality

https://doi.org/10.5194/egusphere-2025-3469
Preprint. Discussion started: 29 July 2025

controlled Surface Ocean CO2 Atlas (SOCAT), Earth Syst. Sci. Data, 5, 125-143, doi:10.5194/essd-5-125-2013, 2013

Orr, J. C., Epitalon, J.-M., Dickson, A. G., and Gattuso, J.-P.: Routine uncertainty propagation for the marine carbon dioxide system, Marine Chemistry, Vol. 207, 84-107, doi:10.1016/j.marchem.2018.10.006, 2018.

Poisson, A., Metzl, N., Brunet, C., Schauer, B., Bres, B., Ruiz-Pino, D., and Louanchi, F.: Variability of sources and sinks of CO2 in the western Indian and southern oceans during the year 1991, J. Geophys. Res., 98(C12), 22759– 22778, doi:10.1029/93JC02501, 1993

Revelle, R., and Suess, H.E.: Carbon dioxide exchange between atmosphere and ocean and the question of an increase of atmospheric CO2 during the past decades. Tellus 9, 18–27. https://doi.org/10.1111/j.2153-3490.1957.tb01849.x, 1957

Sarmiento, J.L., Johnson, K.S., Arteaga, L.A., Bushinsky, S.M., Cullen, H.M., Gray, A.R., Hotinski, R.M., Maurer, T.L., Mazloff, M.R., Riser, S.C., Russell, J.L., Schofield, O.M., Talley, L.D., The Southern Ocean Carbon and Climate Observations and Modeling (SOCCOM) project: A review, Progress in Oceanography, doi: https://doi.org/10.1016/j.pocean.2023.103130, 2023.

Schlitzer, R., 2018. Ocean Data View, http:/odv.awi.de.

Schönberg, C.H.L., Fang, J.K.H., Carreiro-Silva, M., Tribollet, A., Wisshak, M.: Bioerosion: the other ocean acidification problem. ICES (Int. Counc. Explor. Sea) J. Mar. Sci. fsw254 https://doi.org/10.1093/icesjms/fsm254, 2017

Strahl, J., Stolz, I., Uthicke, S., Vogel, N., Noonan, S. H. C., Fabricius, K. E.: Physiological and ecological performance differs in four coral taxa at a volcanic carbon dioxide seep. COMPARATIVE BIOCHEMISTRY AND PHYSIOLOGY A-MOLECULAR & INTEGRATIVE PHYSIOLOGY, 184, 179-186,, 10.1016/j.cbpa.2015.02.018, 2015

Takahashi, T., Olafsson, J., Goddard, J. G., Chipman, D. W., and Sutherland, S. C.: Seasonal variation of CO2 and nutrients in the high-latitude surface oceans: A comparative study, Global Biogeochem. Cycles, 7(4), 843– 878, doi:10.1029/93GB02263, 1993

Takahashi, T., Sutherland, S. C., Sweeney, C., Poisson, A., Metzl, N., Tilbrook, B., Bates, N.,Wanninkhof, R., Feely, R. A., Sabine, C., Olafsson, J., and Nojiri, Y.: Global Sea-Air CO2 Flux Based on Climatological Surface Ocean pCO2, and Seasonal Biological and Temperature Effect, Deep-Sea Res. Pt. II, 49, 9–10, 1601–1622, https://doi.org/10.1016/S0967-0645(02)00003-6, 2002.

Ternon, J.-F., Noyon, M., Penven, P., Herbette, S., Artigas, L. F., Toullec, J., et al.: Resilience – fRonts, EddieS and marIne LIfe in the wEstern iNdian oCEan. In 19 April–24 May 2022, MD237 R/V marion Dufresne (Tech. Rep.). Cruise report, 107 pp., https://doi.org/10.17600/18001917, 2023

Tilbrook, B., E. B. Jewett , M. D. DeGrandpre, J. M. Hernandez-Ayon, , R. A. Feely, D. K. Gledhill, L. Hansson, K. Isensee, M. L. Kurz, J. A. Newton, S. A. Siedlecki, F. Chai, S. Dupont, M. Graco, E. Calvo, D. Greeley, L. Kapsenberg, M. Lebrec, C. Pelejero, K. L. Schoo, M. Telszewski:. An Enhanced Ocean Acidification Observing Network: From People to Technology to Data Synthesis and Information Exchange. Frontiers in Marine Science, 6, 337, DOI:10.3389/fmars.2019.00337, 2019

Touratier, F., Azouzi, L., Goyet, C.: CFC-11, Δ14C and 3H tracers as a means to assess anthropogenic CO2 concentrations in the ocean. Tellus B, 59(2), 318–325, doi:10.1111/j.1600-0889.2006.00247.x, 2007.

https://doi.org/10.5194/egusphere-2025-3469
Preprint. Discussion started: 29 July 2025

1162 Tribollet, A., C. Godinot, M. Atkinson, and C. Langdon: Effects of elevated pCO2 on dissolution of
1163 coral carbonates by microbial euendoliths, Global Biogeochem. Cycles, 23, GB3008,
1164 doi:10.1029/2008GB003286, 2009
1165
1166 Tribollet, A., Chauvin, A., Cuet, P.: Carbonate dissolution by reef microbial borers: a biogeological
1167 process producing alkalinity under different pCO2 conditions. Facies 65, 2.
1168 https://doi.org/10.1007/s10347-018-0548-x, 2019
1169
1170 Uppström, L. R., 1974. The boron/chlorinity ratio of deep-sea water from the Pacific Ocean, Deep Sea
1171 Research and Oceanographic Abstracts, 21, 161–162, https://doi.org/10.1016/0011-7471(74)90074-
1172 6.
1173